A Spectral Study of a Radio-Frequency Plasma-Generated Flux of Atomic Oxygen

Carmen E. Batten
Langley Research Center • Hampton, Virginia

Kenneth G. Brown and Beverley W. Lewis
Old Dominion University • Norfolk, Virginia

The use of trademarks or names of manufacturers in this report is for accurate reporting and does not constitute an official endorsement, either expressed or implied, of such products or manufacturers by the National Aeronautics and Space Administration.

Abstract

The active environment of a radio-frequency (RF) plasma generator, with and without low-pressure oxygen, has been characterized through the identification of emission lines in the spectral region from 250 to 900 nm. The environment is shown to be dependent on the partial pressure of oxygen and the power applied to the RF generator. Atomic oxygen has been found in significant amounts as well as atomic hydrogen and the molecular oxygen species $O_2(^1\Sigma)$. The only charged species observed was the singly charged molecular ion O_2^+. With a polymer specimen in the plasma chamber, carbon monoxide was also observed. The significance of these observations with respect to previous studies using this type of generator to simulate material degradation in space is discussed. The possibility of using these generators as atomic oxygen sources in the development of oxygen atom fluorescence sensors is explored.

Introduction

Radio-frequency (RF) generators have been used by several groups for the generation of oxygen atoms in order to study the oxygen degradation of materials in a simulated low-Earth-orbit (LEO) environment. (See refs. 1–5.) The rate of degradation in these facilities is much greater (by as much as a factor of 7) than that observed in LEO (ref. 1). One possible explanation of this higher rate of degradation is the interaction of the material with the reaction products, which further degrade the material (ref. 4). Such a mechanism would not be possible in LEO because the products are being continuously removed in what is essentially an open system in contrast to the semiclosed, low-flow system present in the RF generator studies. The studies in reference 4 were conducted in the afterglow region of the RF generator in an effort to isolate the sample from other possible deleterious effects of the RF environment such as ultraviolet (UV) radiation and free electrons.

The studies in reference 4 do not rule out the possible presence of other interfering species that might also enhance the reaction rate and provide an additional explanation of the discrepancy between laboratory studies and LEO results. These species are generated by the RF discharge and can still be present in the afterglow region. In this paper we determined the chemical nature of some of these species and what, if any, effect they might have in the overall degradation reaction. We are limited by experimental design to those species that have emission spectra between the wavelengths of 250 and 900 nm. The ultimate goal of this investigation was to understand the dominant processes in an RF-generated plasma and to determine if an RF generator can be used in the development of fluorescence sensors for the detection of atomic and molecular species in LEO and in other rarefied low-flow environments.

Experimental Methods

The experimental system (fig. 1) consisted of a fused quartz cylindrical reaction chamber with two semicircular electrodes surrounding the chamber. An RF generator with associated tuning circuits provided up to 100 W of power at 13.56 MHz. The chamber was evacuated with an external pump. The internal pressure was controlled between 13 and 54 Pa, depending upon the adjustable flow rate of the entering gases. The chamber was provided with a removable flat window at one end, and an optical fiber bundle was located in front of this window. The other end of the fiber bundle was placed at the entrance slit of a single-beam monochromator, and then the fiber bundle acted as a waveguide for the light emitted by the RF chamber. The monochromator had a 1-m path length with an effective aperture of $f/8.7$. The detector was a photomultiplier tube and the resultant signal was amplified and then digitized for computer storage and subsequent analysis.

The gas mixtures were controlled by an external metering and mixing system. The emission spectra were determined for a variety of mixtures of oxygen with other gases to characterize the various species formed and the conditions under which they are produced. An early observation was that the discharge was much brighter at low pressures. This intense background made it difficult to discern the presence or absence of discrete molecular and atomic species. To eliminate this background glow we employed a variety of shield configurations, including an aluminum tunnel which surrounded the observation area inside the chamber. This latter design was an attempt

to produce an environment that might emulate the afterglow environment described in reference 4.

A glass rack was also constructed to allow samples to be mounted inside the reaction chamber. This rack was constructed so that the front face of the sample was held perpendicular to the observation axis of the fiber bundle. As a reference, we used Du Pont Kapton, a material whose oxygen atom degradation has been fully characterized. (See refs. 1 and 5.) Samples were cut into 1-in. squares, weighed prior to being placed in the chamber, and held under vacuum overnight. The samples were then exposed to the plasma for a period of time while the emission spectrum was recorded, after which the samples were removed from the reaction chamber and reweighed to determine the net weight loss. A mass-normalized mass-rate loss (D_1) could then be determined as

$$D_1 = \frac{\Delta m}{m_o t} \; \text{min}^{-1} \qquad (1)$$

where m_o denotes the original mass, Δm denotes the mass loss, and t denotes the time (given in minutes). The values of D_1 could be compared for all the gas mixtures. The mass loss of the material normalized by the exposed sample area (D_2), is defined as

$$D_2 = \frac{D_1 m_o}{2A} \; \frac{g}{\text{cm}^2\text{- min}} \qquad (2)$$

where A denotes the sample area. The factor of 2 occurs in the denominator because both faces of the sample were exposed. The sample is so thin (≈ 1 mil) that collisions with the edges could be ignored. The oxygen atom flux, which is the number of oxygen atoms colliding with the surface per second, is shown in equation (3) as

$$J_0 = \frac{D_2}{\rho(3 \times 10^{-24})} \; \frac{\text{atoms}}{\text{cm}^2\text{- min}} \qquad (3)$$

where J_0 denotes the oxygen atom flux and ρ denotes the sample density. Here, J_0 is computed by using a reaction efficiency (3×10^{-24} cm^3/atom) quoted in reference 1 from LEO data.

Results and Discussion

The main spectral features observed from O_2 plasma in the reaction chamber at low O_2 pressures (17 Pa) are shown in figure 2. The two strong features due to atomic oxygen are at 777 and 845 nm (ref. 6). These two features persist under all experimental conditions with the 845-nm peak becoming very difficult to observe at the lowest pressures

of oxygen. The other pronounced features are the strong band at approximately 656 nm and a weaker feature at 486 nm (not shown in fig. 2), both of which are due to the presence of atomic hydrogen. The 656-nm band persists under all experimental conditions and arises from either residual adsorbed water or surface hydroxyl groups.

As the pressure of oxygen changed, other strong features began to appear in the spectrum. The spectral changes that occurred as the O_2 pressure (p) varied from 32 to 16 Pa are summarized in figures 3 and 4 for the species $O_2(^1\Sigma)$, $O(^3P)$, and O_2^+ (refs. 6 and 7). The molecular feature centered at approximately 760 nm is due to the presence of $O_2(^1\Sigma)$ (ref. 6). This feature persisted as a typical molecular band with structure until the oxygen pressure decreased below 23 Pa. At lower pressures of O_2, some new molecular features emerged, shown in figure 4, at 523 and 557 nm. These features persisted throughout the low-pressure range and are assigned to O_2^+. When the concentration of O_2 was varied by diluting the gas with helium, the O_2^+ features reappeared at low partial pressures of oxygen (i.e., less than 19 Pa) as shown in figure 5. The disappearance of the singlet O_2 species when the gas was diluted with helium paralleled that of the pure gas when the 760-nm band disappeared at O_2 pressures below 23 Pa (fig. 3).

The presence of hydrogen emission lines was independent of any gas mixture examined. After the chamber had been exposed to ambient conditions, the hydrogen line was quite strong and decreased gradually, but it never disappeared. The hydrogen emission was quite likely the result of environmental contamination, with the first strong occurrence due to loosely associated water and the long-term hydrogen emission due to bound water and hydroxyl groups located upon the surface of the chamber.

When the reference material Kapton was placed in the chamber and exposed to the RF field in the presence of O_2, spectra similar to those shown in figure 6 were observed. They were, in basic features, similar to those observed for the chamber with only oxygen present, except that no spectral feature assignable to singlet oxygen $O_2(^1\Sigma)$ was observed at any pressure of O_2. Apparently, those bands that are assignable to O_2^+ persisted to higher pressures of oxygen. This assignment was difficult to make because of overlapping CO emission bands, which are due to the presence of oxidation products of Kapton. The CO bands, however, have a different shape from the bands due to O_2^+; at lower pressures, the CO bands can be distinguished and uniquely assigned at 519, 483, and 451 nm (ref. 7). A CO band also occurs

at 559 nm, but it is obscured by the coincident O_2^+ band. As might be expected, we also observed a significant increase in the hydrogen feature at 486 nm due, in part, to the increased presence of H_2O as an oxidation product in the chamber. The observed assignable plasma bands for the empty chamber and for the chamber with Kapton in place are summarized in table I.

Table I. Assignable Bands in RF Plasma Chamber From References 5 and 6

Species	Spectral lines, nm	
	Without Kapton	With Kapton
O	615, 777, 845	615, 777, 845
$O_2(^1\Sigma)$	760	Absent
O_2^+	523, 557, 635	523, 557, 635
H	486, 656	486, 656
CO	Absent	451, 483, 519, 559
H_2O	Absent	822, 900

From the measured weight loss, we can determine an effective oxygen atom concentration in the reaction chamber by assuming a Kapton erosion efficiency of 3×10^{-24} cm^3/O atom (ref. 1). Figure 7 shows that the value of D_1, normalized by the O_2 partial pressure, varied for different mixtures of gases in the chamber. The line intensity and therefore the oxygen atom density also depended on RF power, as shown in figure 8. However, above 50-W RF power, the emission line strength did not change significantly, thus indicating that we were operating in a power regime where oxygen atom production reached a plateau and was not sensitive to variations in power. Therefore, we determined an average oxygen atom density of approximately 10^{12} O atoms/cm^3 at an RF power of 100 W. This average density is much higher than the atomic oxygen density determined in LEO at 200 km (10^9 O atoms/cm^3) and at 400 km (10^8 O atoms/cm^3) (ref. 8). It is also important to note that the density was determined at a chamber pressure of approximately 40 Pa in pure oxygen. As shown in figure 9, atomic oxygen density increased at compositions below 10 percent O_2 in He.

Concluding Remarks

A technique has been developed to characterize the production of atomic oxygen by using a radio-frequency (RF) generator. This system can be used in future studies of candidate fluorescent materials for the detection of atomic oxygen. The generator has been characterized to enable a determination of the amount of atomic oxygen produced under a variety of experimental conditions. Other species ($O_2(^1\Sigma)$, O_2^+, and H) were also observed that may react with materials in the chamber and interfere with fluorescence studies on candidate materials. Possibly, these other species could, in part, account for the high polymer degradation rates produced in ground experiments when compared with the degradation rates observed in a low Earth orbit (LEO).

References

1. Koontz, S. L.; Albyn, K.; and Leger, L.: Materials Selection for Long Life in Low Earth Orbit—A Critical Evaluation of Atomic Oxygen Testing With Thermal Atom Systems. *J. IES*, vol. 33, Mar.–Apr. 1990, pp. 50–59.

2. Hansen, R. H.; Pascale, J. V.; De Benedictis, T.; and Rentzepis, P. M.: Effect of Atomic Oxygen on Polymers. *J. Polym. Sci.: Part A*, vol. 3, 1965, pp. 2205–2214.

3. Lerner, N. R.; and Wydeven, T.: Polymer Etching in the Oxygen Afterglow—Increased Etch Rates With Increased Reactor Loading. *J. Electrochem. Soc.*, vol. 136, May 1989, pp. 1426–1430.

4. Lerner, N. R.; and Wydeven, T.: Decrease in the Etch of Polymers in the Oxygen Afterglow With Increasing Gas Flow Rate. *J. Appl. Polym. Sci.*, vol. 35, 1988, pp. 1903–1908.

5. Miller, W. L.: *Mass Loss of Shuttle Space Suit Orthofabric Under Simulated Ionospheric Atomic Oxygen Bombardment.* NASA TM-87149, 1985.

6. Weast, Robert C.; and Astle, Melvin J.: *CRC Handbook of Chemistry and Physics.* 60th ed., CRC Press, 1979.

7. Pearse, R. W. B.; and Gaydon, A. G.: *The Identification of Molecular Spectra*, Third ed., Chapman & Hall, Ltd., 1963.

8. Peplinski, D. R.; Arnold, G. S.; and Borson, E. N.: Introduction to Simulation of Upper Atmosphere Oxygen Satellite Exposed to Atomic Oxygen in Low Earth Orbit. *Thirteenth Space Simulation Conference—The Payload: Testing For Success*, J. Stecher, ed., NASA CP-2340, 1984, pp. 133–145.
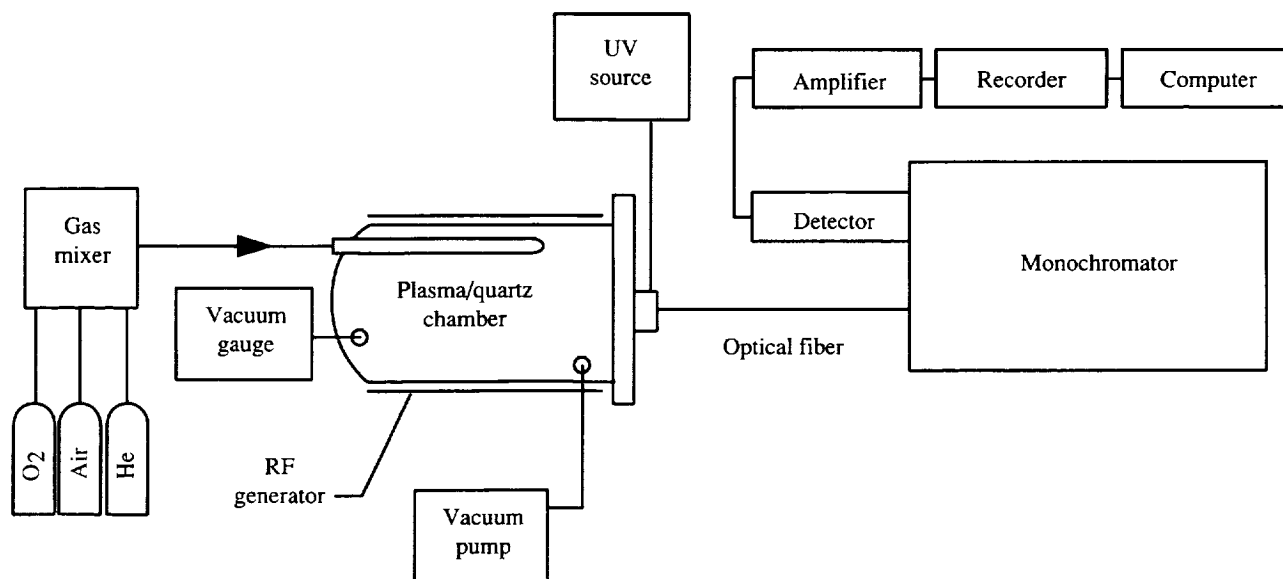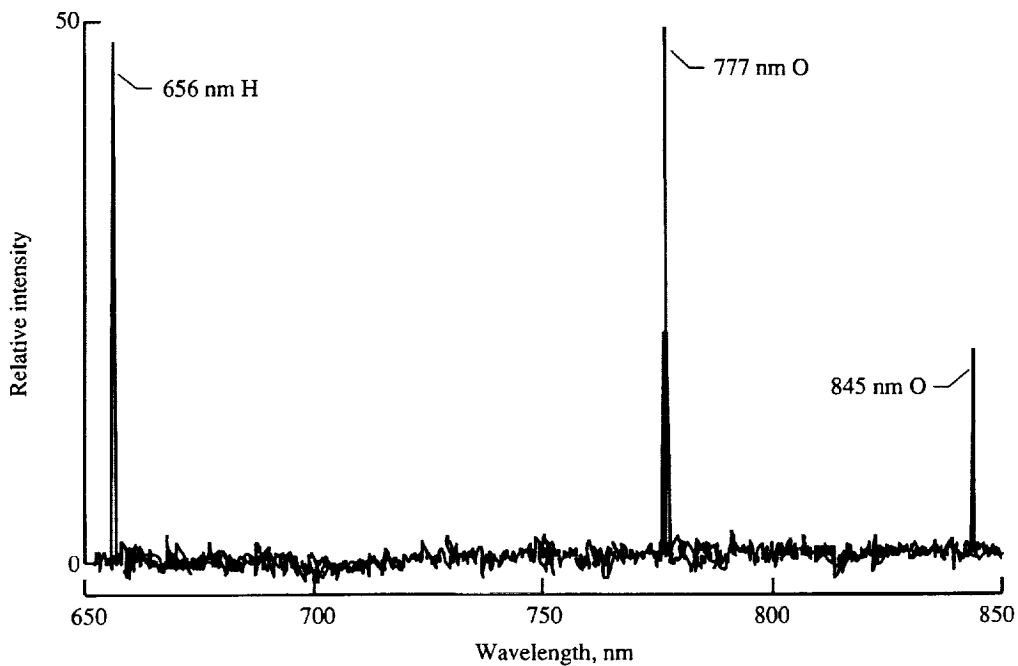
4

Figure 1. Sensor evaluation system.

Figure 2. Identification of spectral lines for atomic O and H. Pure oxygen with no sample in chamber; $p = 17$ Pa.
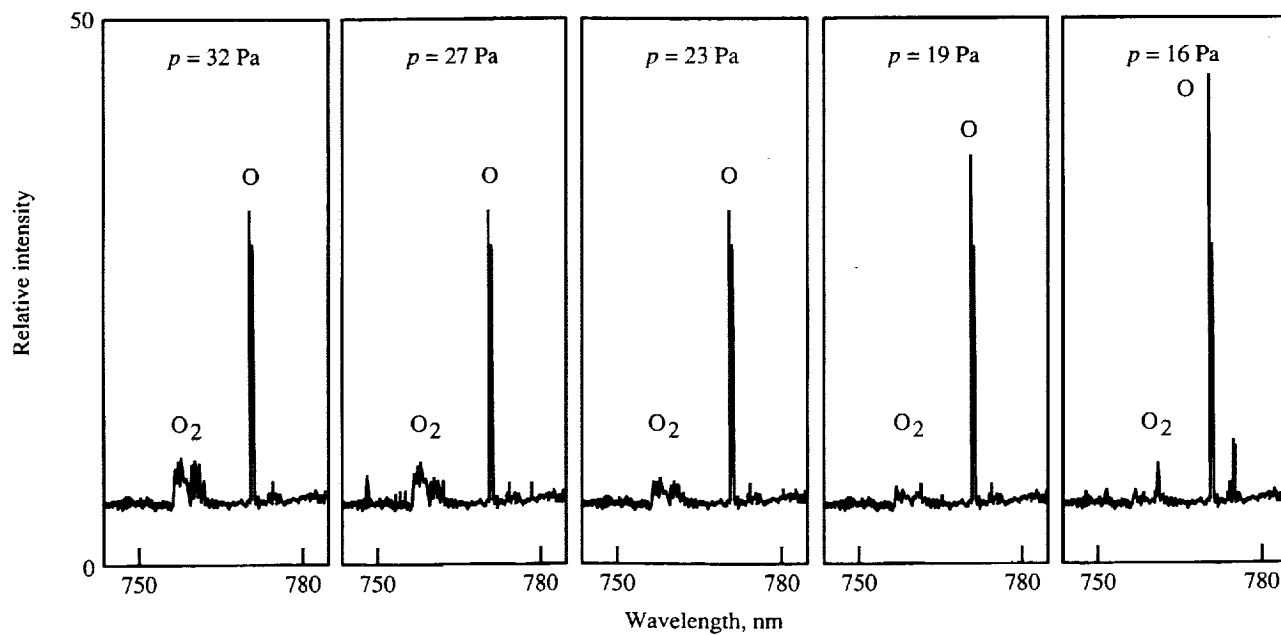

Figure 3. Pressure dependence of $O_2(^1\Sigma)$ and $O(^3P)$ in 100-percent oxygen plasma
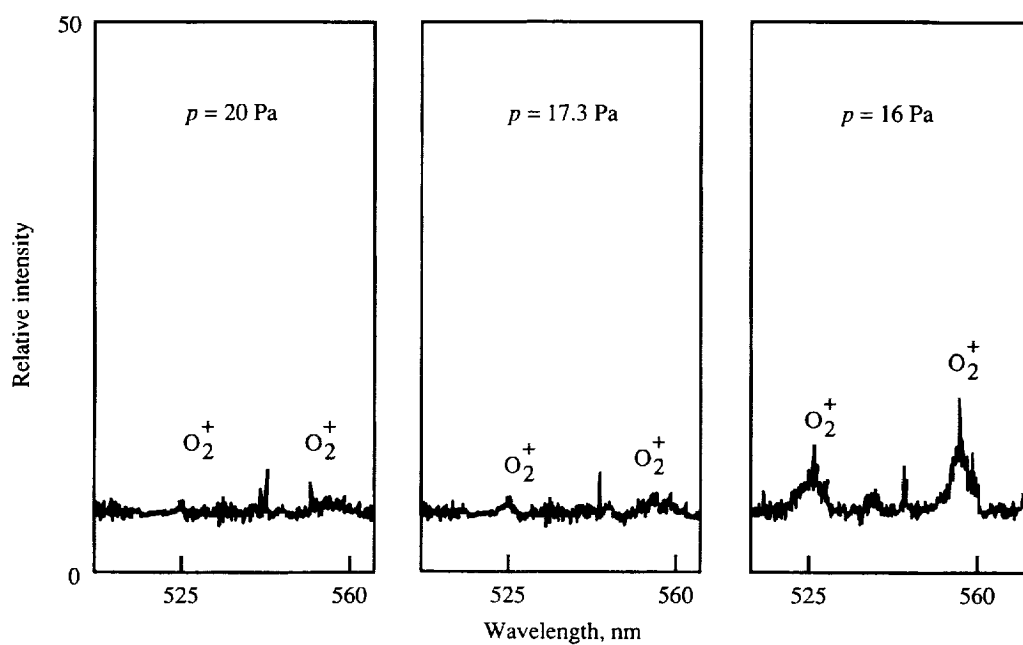
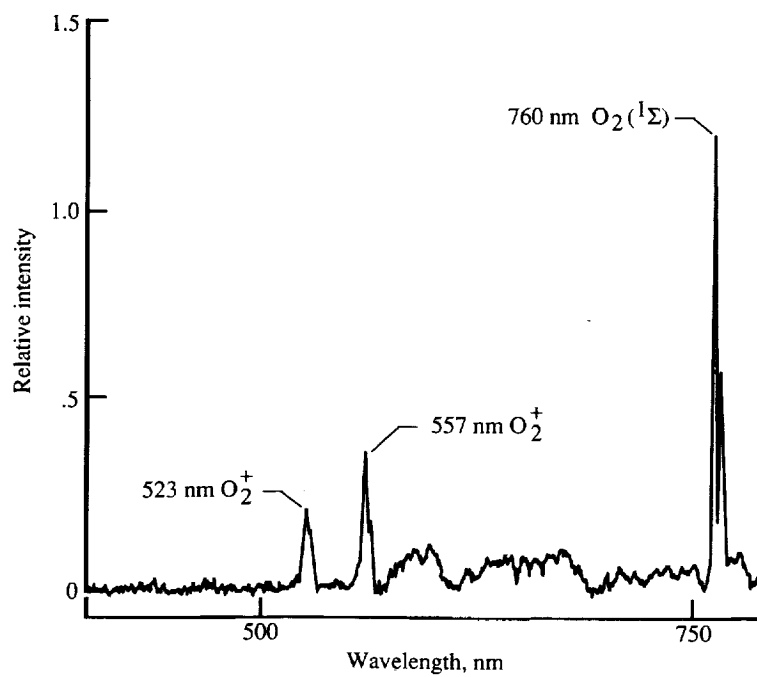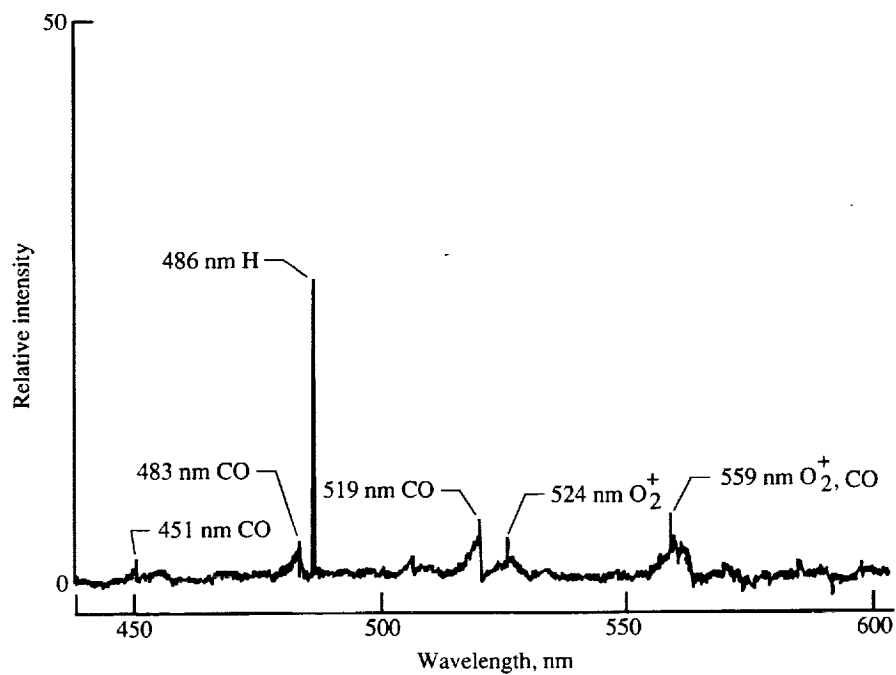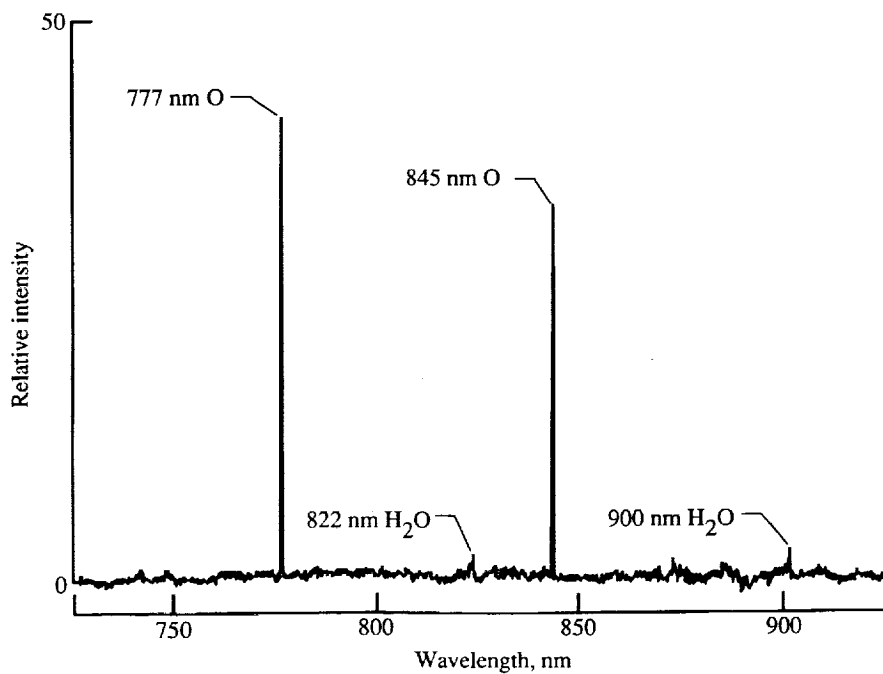Figure 4. Pressure dependence of O_2^+ in 100-percent oxygen plasma.

Figure 5. Molecular oxygen species in 40-percent oxygen in helium plasma with a total pressure of 49.3 Pa.

(a) Range of wavelength from 450 to 600 nm.

(b) Range of wavelength from 750 to 900 nm.

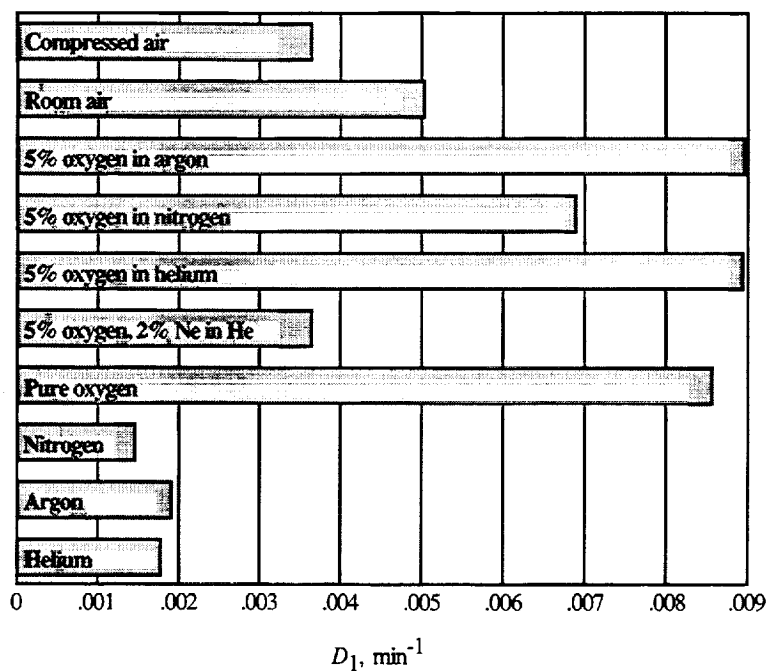Figure 6. Spectrum of oxygen plasma with Kapton in chamber.

8

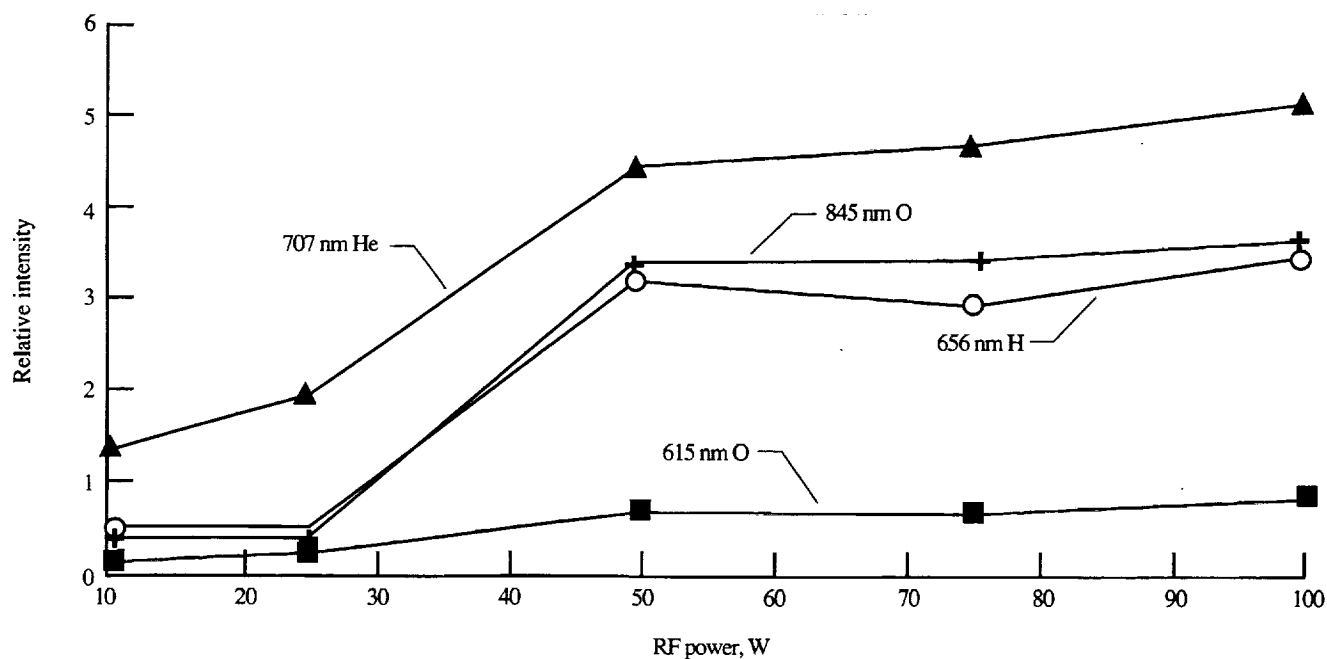Figure 7. Kapton weight-loss rate (D_1) corrected for pressure.

Figure 8. Effect of RF power on emission lines of a mixture of 50 percent O_2 in He. $p = 33.3$ Pa; flow rate is 5.00 standard cm^3/min.

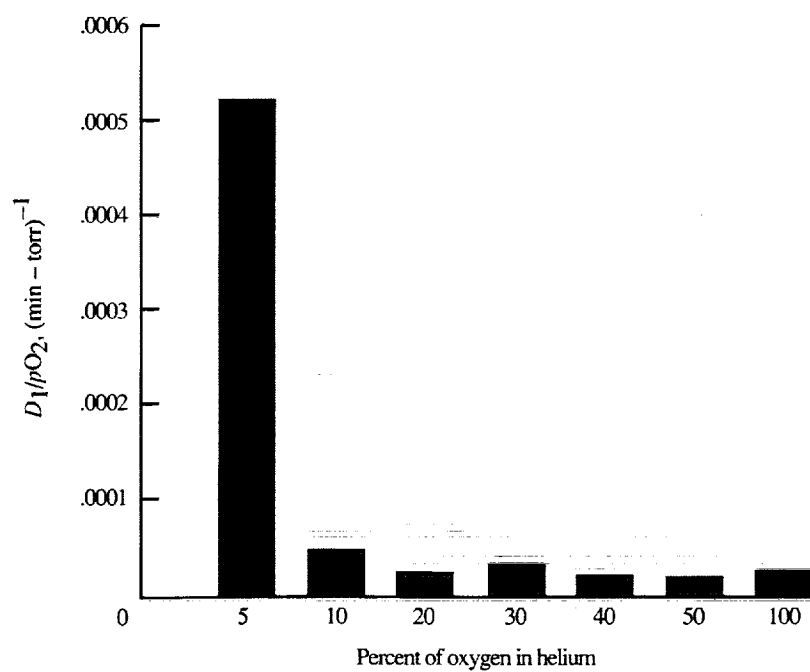Figure 9. Effect of O_2 pressure in the plasma on weight-loss rate of Kapton.

REPORT DOCUMENTATION PAGE

Public reporting burden for this collection of information is estimated to average 1 hour per response, including the time for reviewing instructions, searching existing data sources, gathering and maintaining the data needed, and completing and reviewing the collection of information. Send comments regarding this burden estimate or any other aspect of this collection of information, including suggestions for reducing this burden, to Washington Headquarters Services, Directorate for Information Operations and Reports, 1215 Jefferson Davis Highway, Suite 1204, Arlington, VA 22202-4302, and to the Office of Management and Budget, Paperwork Reduction Project (0704-0188), Washington, DC 20503.

1. AGENCY USE ONLY(Leave blank)	2. REPORT DATE December 1994	3. REPORT TYPE AND DATES COVERED Technical Memorandum

4. TITLE AND SUBTITLE

A Spectral Study of a Radio-Frequency Plasma-Generated Flux of Atomic Oxygen

5. FUNDING NUMBERS

WU 307-51-12-04

6. AUTHOR(S)

Carmen E. Batten, Kenneth G. Brown, and Beverley W. Lewis

7. PERFORMING ORGANIZATION NAME(S) AND ADDRESS(ES)

NASA Langley Research Center
Hampton, VA 23681-0001

8. PERFORMING ORGANIZATION REPORT NUMBER

L-17351

9. SPONSORING/MONITORING AGENCY NAME(S) AND ADDRESS(ES)

National Aeronautics and Space Administration
Washington, DC 20546-0001

10. SPONSORING/MONITORING AGENCY REPORT NUMBER

NASA TM-4612

11. SUPPLEMENTARY NOTES

Batten: Langley Research Center, Hampton, VA; Brown and Lewis: Old Dominion University, Norfolk, VA.

12a. DISTRIBUTION/AVAILABILITY STATEMENT

Unclassified–Unlimited
Subject Category 35
Availability: NASA CASI (301) 621-0390

12b. DISTRIBUTION CODE

13. ABSTRACT *(Maximum 200 words)*

The active environment of a radio-frequency (RF) plasma generator, with and without low-pressure oxygen, has been characterized through the identification of emission lines in the spectral region from 250 to 900 nm. The environment is shown to be dependent on the partial pressure of oxygen and the power applied to the RF generator. Atomic oxygen has been found in significant amounts as well as atomic hydrogen and the molecular oxygen species $O_2(^1\Sigma)$. The only charged species observed was the singly charged molecular ion O_2^+. With a polymer specimen in the plasma chamber, carbon monoxide was also observed. The significance of these observations with respect to previous studies using this type of generator to simulate material degradation in space is discussed. The possibility of using these generators as atomic oxygen sources in the development of oxygen atom fluorescence sensors is explored.

14. SUBJECT TERMS

Radio-frequency plasma; Oxygen atom flux; Spectral analysis

15. NUMBER OF PAGES

11

16. PRICE CODE

A03

17. SECURITY CLASSIFICATION OF REPORT Unclassified	18. SECURITY CLASSIFICATION OF THIS PAGE Unclassified	19. SECURITY CLASSIFICATION OF ABSTRACT Unclassified	20. LIMITATION OF ABSTRACT